

Article

Selective Separation of Fluorite from Scheelite Using *N*-Decanoylsarcosine Sodium as a Novel Collector

Zekun Miao ¹, Liming Tao ¹, Jianjun Wang ¹, Zheyi Jiang ¹, Tao Peng ¹, Wei Sun ^{1,2,3} and Zhiyong Gao ^{1,2,3,*} 

¹ School of Minerals Processing and Bioengineering, Central South University, Changsha 410083, China; miaozeekun@csu.edu.cn (Z.M.); taoliming@csu.edu.cn (L.T.); wangjianjuncsu@126.com (J.W.); jiangzheyi@csu.edu.cn (Z.J.); 215611039@csu.edu.cn (T.P.); swcsu163@163.com (W.S.)

² Key Laboratory of Hunan Province for Clean and Efficient Utilization of Strategic Calcium-Containing Mineral Resources, Central South University, Changsha 410083, China

³ Hunan International Joint Research Center for Efficient and Clean Utilization of Critical Metal Mineral Resources, Central South University, Changsha 410083, China

* Correspondence: zhiyong.gao@csu.edu.cn

Abstract: Fluorite and scheelite, which are strategic calcium-bearing minerals, have similar active sites (Ca²⁺); as a result, the efficient separation of the two minerals is still one of the world's most difficult problems in the field of flotation. In this work, *N*-decanoylsarcosine sodium (SDAA), a non-toxic and low-cost amino acid surfactant, was applied in the flotation separation of fluorite from scheelite for the first time. In the test, single mineral, binary mixed minerals, and actual ore experiments showed that the pre-removal of fluorite from scheelite by reverse flotation can be achieved. The results of adsorption capacity detections, zeta potential tests, and FTIR analysis showed that the negatively charged SDAA prefers to adsorb onto the positively charged fluorite surface due to the electrostatic interaction. The results of crystal chemistry and DFT calculations showed that SDAA has a stronger chemical interaction and more electron transfer numbers to the Ca atom on the fluorite surface and forms a Ca-SDAA complex. Therefore, the significant difference in the adsorption behavior of SDAA on the surfaces of two minerals provided a new insight into the separation efficiency of amino acids and possesses a great potential for industrial application in scheelite flotation.

Keywords: scheelite; fluorite; flotation; *N*-decanoylsarcosine sodium; collector



Citation: Miao, Z.; Tao, L.; Wang, J.; Jiang, Z.; Peng, T.; Sun, W.; Gao, Z. Selective Separation of Fluorite from Scheelite Using *N*-Decanoylsarcosine Sodium as a Novel Collector. *Minerals* **2022**, *12*, 855. <https://doi.org/10.3390/min12070855>

Academic Editors: Wengang Liu and Saeed Chehreh Chelgani

Received: 12 May 2022

Accepted: 1 July 2022

Published: 4 July 2022

Publisher's Note: MDPI stays neutral with regard to jurisdictional claims in published maps and institutional affiliations.



Copyright: © 2022 by the authors. Licensee MDPI, Basel, Switzerland. This article is an open access article distributed under the terms and conditions of the Creative Commons Attribution (CC BY) license (<https://creativecommons.org/licenses/by/4.0/>).

1. Introduction

Scheelite and fluorite, as the main sources of tungsten and fluorine, are considered important strategic mineral resources [1]. Tungsten is widely used in metallurgical machinery, the petrochemical industry, aerospace, and national defense [2]. Fluorine is widely used in refrigeration, pesticide, flux, and other industries [3]. Low-grade co-associated scheelite and fluorite, as important mineral resources, have had more and more attention paid to their development and utilization with the decrease of high-grade scheelite and fluorite.

Scheelite and fluorite are dilute soluble salt minerals with natural hydrophilicity and high energy in an aqueous solution [4,5]. Foam flotation is the most commonly used method for separating fluorite and scheelite, but it is difficult to separate them well due to their similar physical and chemical properties [6]. Therefore, the content of fluorite in the scheelite concentrate used in industry is high, and the quality of scheelite concentrate often fails to meet the product standard.

At present, the main separation method of scheelite and fluorite in the industry is the high alkali method. Scheelite was preferred for flotation by adding a large amount of sodium silicate (SS) to depress fluorite [7,8]. Then, fluorite was activated from the tungsten tailings. However, this method has a strong depressant effect on fluorite by adding a large amount of SS in a high alkaline environment [9]. This makes recycling the fluorite tricky, and much of it is lost. In addition, the activation of some gangue minerals makes it

difficult to improve the grade of fluorite concentrate when using floating tungsten tailings for fluorite cleaning [10]. Moreover, most of the research on the flotation separation of scheelite and fluorite mainly focuses on developing efficient and selective depressants (sodium polyacrylate, sodium alginate, diethylenetriaminepentaacetic acid, etc.) to depress the flotation capacity of fluorite, which also inevitably leads to the loss of scheelite [9,11–13].

Reverse flotation of floating fluorite and depressing scheelite may be a better alternative, considering the drawbacks of existing processes [10]. It should be emphasized that fluorite possesses better natural floatability than scheelite, leading to the possibility to separate fluorite from scheelite by reverse flotation [14–17]. However, the Ca active sites on fluorite and scheelite are similar, which makes them difficult to separate by flotation [8,18,19]. Moreover, it is better not to use scheelite depressants since they inevitably lead to the loss of fluorite in reverse flotation. Thus, a green collector with higher selectivity and higher efficiency for fluorite against scheelite should be developed.

N-decanoylsarcosine sodium (SDAA), as a carboxyl and amide-based amino acid surfactant that is non-toxic and has high hydrophobicity and good biodegradability, is widely used in the field of care, food additives, biological products, drug preparation, etc. [20–22]. It was attempted to use SDAA as a novel fluorite collector due to its distinguished properties of high-quality and long-lasting foam. In this work, SDAA was used as a novel collector for the selective separation of fluorite from scheelite through the flotation tests of single mineral and binary mixed minerals. The adsorption mechanism of SDAA or NaOL on both minerals was studied by total organic carbon (TOC) tests, zeta potential tests, Fourier transform infrared spectroscopy (FTIR) analysis, and density functional theory (DFT) calculations.

2. Materials and Methods

2.1. Materials and Reagents

Pure scheelite and fluorite samples were purchased from Chenzhou, China, and then smashed with a hammer and ground in a porcelain mill. Subsequently, $-4 + 35 \mu\text{m}$ fractions screened by a Tyler sieve were collected for flotation tests and $-2 \mu\text{m}$ fractions were prepared for zeta potential and FTIR measurements. X-ray diffraction measurements and chemical analysis showed that the purity of both scheelite and fluorite was above 98%.

The sample of actual scheelite ore (containing fluorite) for flotation tests was obtained from the Chenzhou tungsten mine of Hunan Province, China. The sample was wet ground to 71 wt.% passing $74 \mu\text{m}$ with a ball mill. Chemical analysis showed that the grade of WO_3 and CaF_2 in the actual ore sample was 0.30% and 18.72%, respectively.

HCl and NaOH solutions were used to regulate the pulp pH. Analytically pure *N*-decanoylsarcosine (SDAA) and sodium oleate (NaOL) were provided by Shanghai Aladdin Bio-Chem Technology Co., LTD, Shanghai, China. All experiments were conducted using deionized water with a resistivity of over $18 \text{ M}\Omega \times \text{cm}$.

2.2. Flotation Tests

Flotation experiments of the single mineral and mixed binary minerals were carried out in an XFG_{II} flotation machine with a 40 mL plexiglass cell at an impeller speed of 1700 r/min. In each experiment, 2.0 g of single or binary mixed minerals (1.0 g scheelite and 1.0 g fluorite) samples were added to the plexiglass cell with 35 mL of deionized water. After adding desired reagents and agitating for 3 min, the slurry pH was adjusted by HCl and NaOH, followed by the flotation for 4 min. In single mineral tests, all flotation products were dried and weighed to calculate the flotation recovery. For binary mixed minerals, the concentrates and tailings were weighed and assayed to determine the scheelite grade and calculate the flotation recovery. Three repeated experiments were conducted in this study and the standard deviation was recorded.

Flotation experiments of actual ore were carried out in an XFG-63 flotation machine with a 0.5 L plexiglass cell at an impeller speed of 1900 r/min. In each experiment, 150 g of actual ore samples were added to the plexiglass cell with 350 mL of water. After adding

the desired reagents and agitating for 3 min, the slurry pH was adjusted by HCl and NaOH, followed by the flotation for 4 min. In actual ore tests, the concentrates and tailings were weighed and assayed to determine the scheelite and fluorite grade and calculate the flotation recovery. Three repeated experiments were conducted in this study and the standard deviation was recorded.

2.3. Surface Adsorption Detection

A total organic carbon (TOC) detector (TOC-VepH, Kyoto, Japan) was used to measure the amounts of SDAA or NaOL adsorbed on scheelite and fluorite based on the residual content method [4,23]. The sample treatment method used in the adsorption capacity test process was the same as in the flotation process, except that there was no flotation process. After the pulp was centrifuged, the supernatant was extracted to measure the adsorption capacity. Each experimental test operation was repeated three times, and the mean and standard deviation of the surface adsorption amount were calculated. Hence, the different amounts of SDAA or NaOL adsorbed on the two minerals were calculated by Equation (1) [24]:

$$\Gamma = \frac{(C_i - C_r) \times V}{\eta \times w} \quad (1)$$

where Γ denotes the adsorption density of the flotation reagent on each mineral (mg/g); η denotes the carbon content in the flotation reagent molecule (%); C_r and C_i are individually the contents of residual and initial TOC in the flotation reagent supernatant (mg/L); and V and w denote the flotation reagent volume (L) and the mineral specimen weight (g).

2.4. Zeta Potential Test

The zeta potential values of fluorite and scheelite treated with SDAA or NaOL were measured using a Nano ZS90 analyzer (Malvern Zetasizer, Malvern, UK). Firstly, 0.02 g of the mineral sample was added to 40 mL of KCl (1×10^{-3} mol/L) solution to prepare a mineral particle suspension. Then, the flotation reagents were added in sequence in the flotation process, the pH was adjusted, and the pulp was allowed to stand for 5 min. Finally, the supernatant was extracted for zeta potential value measurement. Each set of experiments was repeated three times, and the mean and standard deviation of zeta potentials were calculated.

2.5. FTIR Measurements

The FTIR spectra were obtained at 25 °C by using a Nexus 670 FTIR spectrometer (Nicolet, WI, USA). Mineral samples of less than 5 μm were initially prepared following the same procedure as the flotation tests except that the final flotation step was omitted. Instead, the mineral suspension was continuously magnetically stirred for 30 min. Then, the samples were washed with deionized water three times, vacuum dried in an oven at 40 °C, and subjected to FTIR analysis [25].

2.6. DFT Calculations

Quantum chemistry calculations were performed using the Cambridge Series Total Energy Packet (CASTEP) modules in Materials Studio 2018 [26,27]. Since the (111) surface of fluorite and (112) surface of scheelite are their common exposed surfaces, the first-principles method of density functional theory calculation was used to establish the crystal structure of SDAA^- and the surfaces of fluorite (111) and scheelite (112), shown in Figure 1 [10,28].

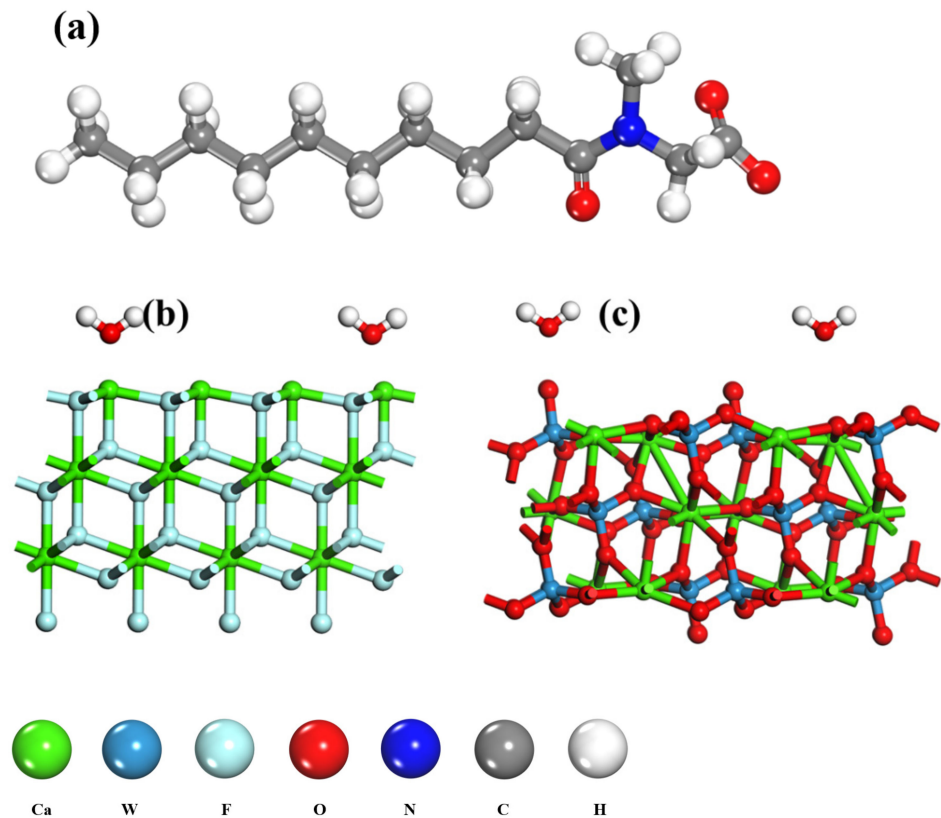


Figure 1. (a) Optimized geometry of SDAA anion slab model; (b) optimized geometry of fluorite slab model; and (c) optimized geometry of scheelite slab model.

Based on the optimized structure of bulk cells, the (111) surface of fluorite was generated by cleaving a plane in the (111) direction at the top of position of 0.0 with 3.0 thickness in the fractional coordination, and the (112) surface of scheelite at the top position of 1.5 with 3.0 thickness. Then, extended supercells were 2×2 (the area was 2.39 nm^2) for fluorite and 2×1 (the area was 2.01 nm^2) for scheelite to meet the area large enough for glucose adsorption. Subsequently, a vacuum of 30 \AA along the Z direction was set.

In the calculation, the Perdew–Burke–Ernzerhof (PBE) functional was used to approximate the exchange-dependent potential of the generalized gradient approximation (GGA) with the plane wave cutoff energy of 517 eV . In volume element optimization, a $1 \times 1 \times 1$ intermediate k-point grid with a Monkhorst–Pack k-point grid was used. The self-consistent field convergence was fixed at $2.0 \times 10^{-6} \text{ eV/atom}$. In the calculation of structural relaxation and energy, the convergence criteria for crystal internal stress, energy, maximum force, and maximum displacement were 0.1 GPa , $2.0 \times 10^{-5} \text{ eV/atom}$, 0.05 eV/\AA , and 0.002 \AA , respectively. The lattice parameters c of fluorite bulk cell after relaxation were 5.553 \AA , 5.553 \AA , and 5.553 \AA , and those of scheelite were 5.310 \AA , 5.310 \AA , and 11.843 \AA . Three water molecules were placed in parallel on both sides of the reagent molecule at a distance of 2.500 \AA from the mineral surface to simulate the aqueous solution environment. The adsorption energy (E_{ads}) is calculated by Equation (2):

$$E_{ads} = E_{system} - (E_{reagent} + E_{surface+water}) \quad (2)$$

where E_{system} is the electronic energy of the total system of the reagent and the mineral surface with water from first-principles calculations and $E_{reagent}$ and $E_{surface+water}$ are the corresponding energies of the reagent and the mineral surface with water, respectively [21,29,30].

3. Results

3.1. Flotation Results of Single Mineral, Binary Mixed Minerals, and Actual Ore

The pulp pH can affect the surface potentials of minerals and the active components of reagents, so the pulp pH is a very important factor in flotation. Moreover, the concentration of the collector has a direct effect on the hydrophobicity of mineral surfaces [31–34]. Therefore, the flotation tests of the single mineral were performed to evaluate the effect of the pulp pH and the concentration of SDAA on the flotation behavior of fluorite and scheelite, as shown in Figures 2 and 3.

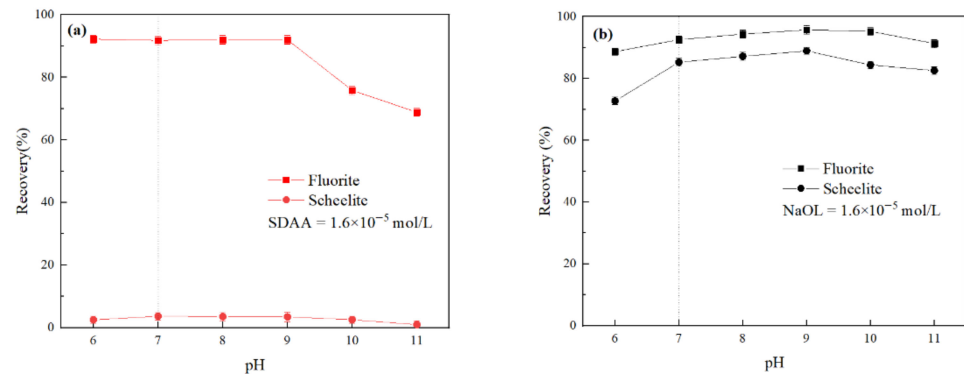


Figure 2. (a) Recoveries of fluorite and scheelite as a function of the pulp pH using SDAA as a collector and (b) recoveries of fluorite and scheelite as a function of the pulp pH using NaOL as a collector.

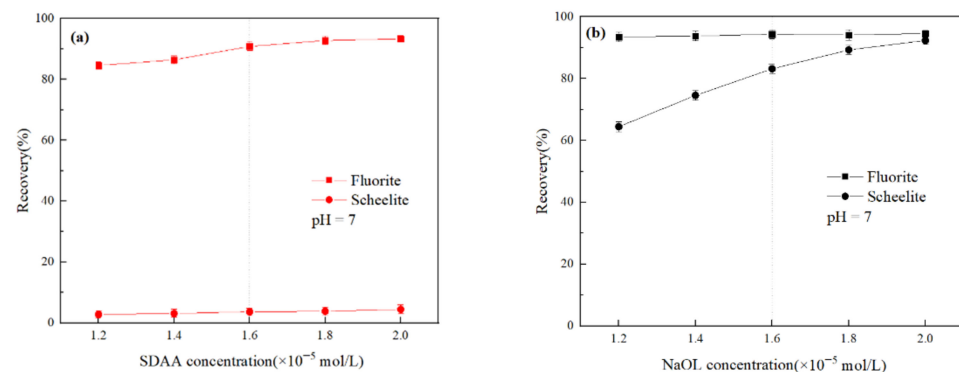


Figure 3. (a) Recoveries of fluorite and scheelite as a function of collector concentration using SDAA as the collector and (b) recoveries of fluorite and scheelite as a function of collector concentration using NaOL as the collector.

As shown in Figure 2 with the increase of pH, the recovery of fluorite using the SDAA collector firstly stabilized and then decreased, and the recovery of scheelite maintained at less than 5%. However, the recoveries of fluorite and scheelite using the NaOL collector were almost above 80%, indicating that NaOL has a low selectivity for the two minerals. The recovery difference between fluorite and scheelite exceeded 88% when the pH was 6.0–8.0. Therefore, a neutral pH of 7.0 was adopted in subsequent experiments.

Figure 3 shows the effect of the concentration of SDAA or NaOL on the fluorite and scheelite recoveries at pH 7.0. It can be seen that the fluorite and scheelite recoveries increased gradually with increasing concentrations of SDAA or NaOL. In particular, when the concentration of the collector was 1.6×10^{-5} mol/L, the recovery of fluorite was over 90% whether using SDAA or NaOL. Moreover, the recovery of scheelite using NaOL (83.16%) was much higher than using SDAA (3.67%), indicating that SDAA had a weaker collecting ability for scheelite than NaOL. Therefore, 1.6×10^{-5} mol/L was selected as the preferred concentration for SDAA.

In order to verify the separation ability of SDAA for fluorite and scheelite, the flotation tests of binary mixed minerals (fluorite: scheelite = 1:1, wt. %) were carried out at the neutral pH 7.0. The results are shown in Figure 4.

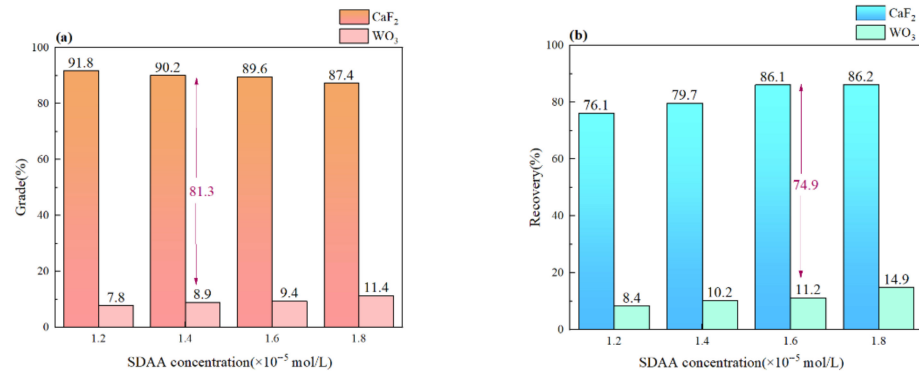


Figure 4. (a) Grade of CaF₂ and WO₃ in fluorite concentrate as a function of SDAA concentration at pH 7.0 in binary mixed mineral tests and (b) recovery of CaF₂ and WO₃ in fluorite concentrate as a function of SDAA concentration at pH 7.0 in binary mixed mineral tests.

With the increasing concentration of SDAA from 1.2×10^{-5} mol/L to 1.8×10^{-5} mol/L, the recovery of fluorite increased gradually, while the grade gradually decreased. The recovery and grade of scheelite were the opposite of fluorite. When the concentration of SDAA was 1.6×10^{-5} mol/L, the grade and recovery of fluorite were 89.6% and 86.1%, respectively. In contrast, scheelite grade and recovery did not exceed 15% at any SDAA concentration. The results indicate that SDAA could effectively achieve the selective separation of fluorite from scheelite without any depressants at a small concentration of 1.4×10^{-5} mol/L.

In order to verify the separation ability of SDAA for fluorite and scheelite, the flotation tests of actual ore were carried out at the neutral pH 7.0 and the concentration of SDAA or NaOL was 100 g/t. The results were shown in Table 1.

Table 1. Grade and recovery of CaF₂ and WO₃ in fluorite concentrate when the concentration of SDAA or NaOL was 100 g/t at pH 7.0 in actual ore tests.

| | Grade of CaF ₂ (%) | Grade of WO ₃ (%) | Recovery of CaF ₂ (%) | Recovery of WO ₃ (%) |
|---------|-------------------------------|------------------------------|----------------------------------|---------------------------------|
| NaOL | 44.02 | 0.53 | 63.80 | 47.93 |
| SDAA | 39.62 | 0.33 | 54.02 | 28.12 |
| Raw ore | 18.72 | 0.30 | / | / |

Table 1 shows that when the pH was at 7.0 and the concentration of NaOL was 100 g/t, the grades of WO₃ and CaF₂ were obviously increased, which means that fluorite and scheelite were enriched into the concentrate at the same time. On the contrary, when the flotation reagent was SDAA, only the grade of CaF₂ in the concentrate was obviously increased, indicating that only fluorite was enriched in the concentrate, while scheelite was hardly enriched in the concentrate. Moreover, the recovery of CaF₂ and WO₃ in the concentrate were obviously different when the flotation reagent was SDAA. The actual flotation tests showed that SDAA can separate fluorite from scheelite without any depressants, while NaOL cannot.

3.2. Surface Adsorption Test Results

In order to quantify the adsorption amounts of SDAA and NaOL on the surfaces of the two minerals, the TOC tester was used to measure SDAA and NaOL when the flotation reagent concentration was 1.6×10^{-5} mol/L and the pH was at 7.0 according to the residual

content method. The results of the adsorption density on the surfaces of the two minerals are shown in Figure 5.

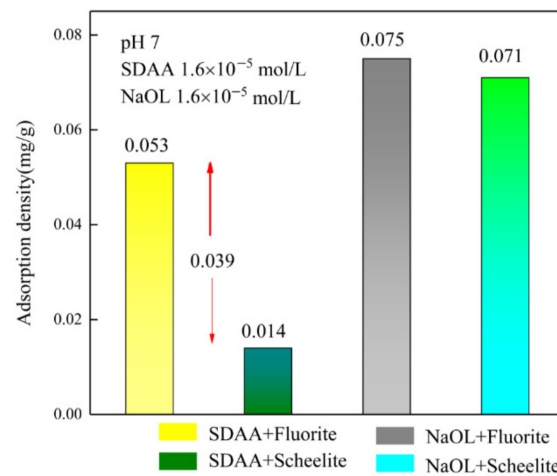


Figure 5. The adsorption density of SDAA and NaOL on the surfaces of the two minerals.

Figure 5 shows that when the pH was at 7.0 and the flotation reagent concentration was 1.6×10^{-5} mol/L, the adsorption densities of NaOL on the surfaces of fluorite and scheelite were 0.075 mg/g and 0.071 mg/g, respectively. The adsorption density of NaOL on the surface of fluorite was slightly higher than that of SDAA (0.053 mg/g), which corresponds to the higher recovery of NaOL than SDAA in the results of the single-mineral flotation test of fluorite. However, the adsorption density of SDAA on the surface of fluorite was significantly greater than that on the surface of scheelite, indicating that SDAA adsorbed more onto the surface of fluorite, while almost no adsorption occurred on the surface of scheelite.

3.3. Zeta Potential Test Results

The zeta potential test can more directly reflect the difference in mineral surface potential and the difference in the adsorption amount of the flotation reagent before and after the adsorption of the flotation reagent [12,35–37]. Therefore, the zeta potential charges were measured when the pH was 7.0 and the concentration of the flotation reagent was 1.6×10^{-5} mol/L. The results before and after the adsorption of SDAA and NaOL on the surfaces of the two minerals are shown in Figure 6.

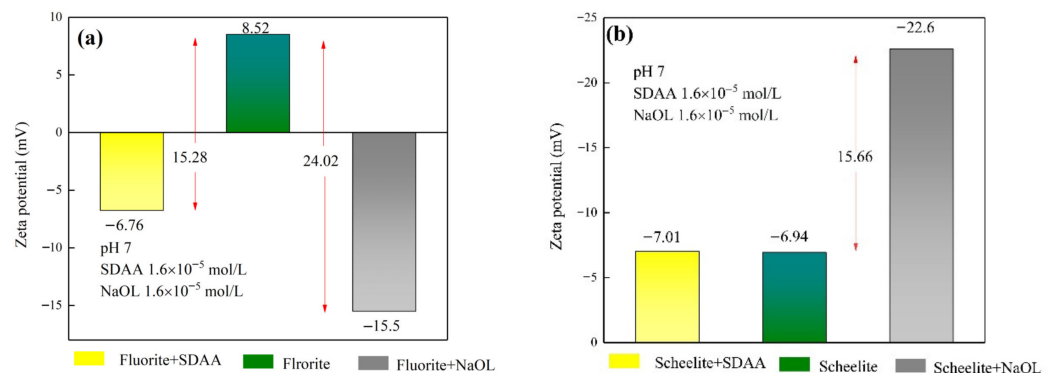


Figure 6. Zeta potentials of fluorite (a) and scheelite (b) with or without treating with SDAA or NaOL.

In Figure 6, the zeta potential of pure fluorite without a collector was 8.52 mV and that of pure scheelite was -6.94 mV, which was almost consistent with the previous investigations [6,38,39]. It can be seen from Figure 6 that when the pH was 7.0 and the

flotation reagent concentration was 1.6×10^{-5} mol/L, the zeta potential values of fluorite and scheelite had a significant negative shift after adding NaOL. Negative shift values for fluorite and scheelite were 24.02 mV and 15.66 mV, respectively, indicating that NaOL strongly adsorbed onto the surfaces of fluorite and scheelite. However, the negative shift value of fluorite (15.28 mV) after adding SDAA was much higher than that of scheelite (0.07 mV), indicating that SDAA strongly adsorbed onto the surface of fluorite but hardly occurred on the surface of scheelite.

3.4. FTIR Analysis Results

FTIR could further reveal the interaction between functional groups of SDAA molecules or NaOL molecules and the two minerals. In order to deeply study the interaction mechanism of SDAA with fluorite and scheelite, the FTIR spectra of fluorite and scheelite before and after SDAA treatment at pH 7.0 were measured, as shown in Figure 7.

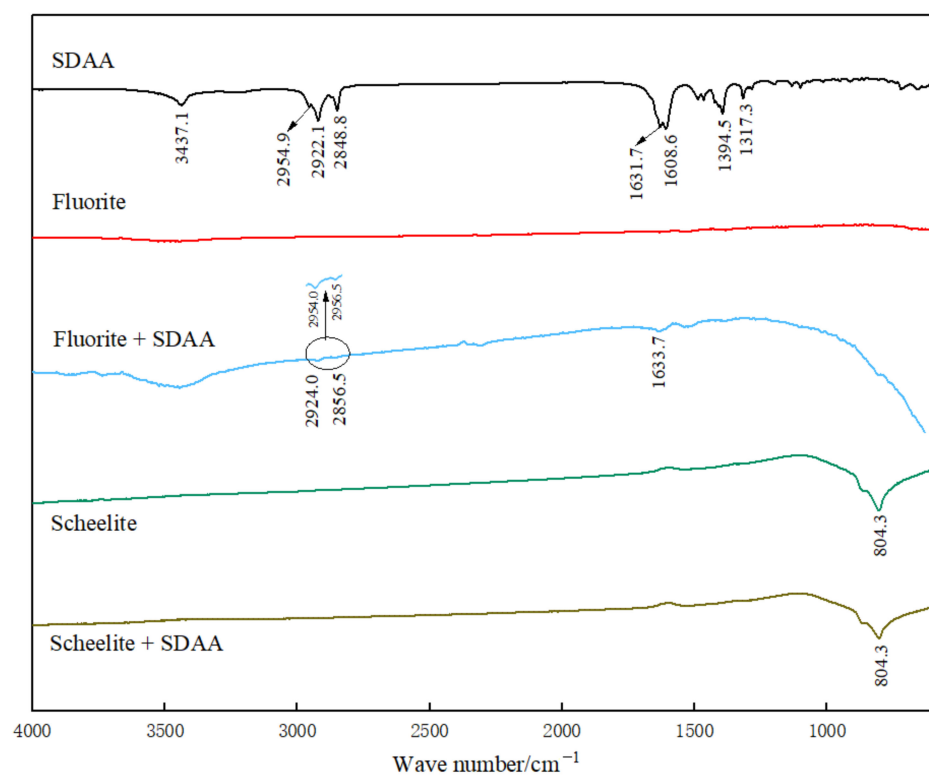


Figure 7. FTIR spectra of SDAA and two minerals before and after the treatment of SDAA.

In the FTIR spectra of SDAA, the peaks at 2922.1 cm^{-1} and 2848.8 cm^{-1} are caused by the stretching vibrations of the $-\text{CH}_2-$ and $-\text{CH}_3-$ groups, respectively [40,41]. The peaks at 1608.6 cm^{-1} and 1394.5 cm^{-1} correspond to the carbonyl stretching vibration of the carboxyl ($-\text{COO}-$) group [42,43]. Another characteristic peak of SDAA appears at 1631.7 cm^{-1} , which is attributed to an amide group ($-\text{CON}-$) stretching vibration [25,44].

In Figure 7, after the SDAA treatment, new bands appeared at 2924.0 cm^{-1} and 2856.5 cm^{-1} in the FTIR spectra of fluorite because of the $-\text{CH}_2-$ and $-\text{CH}_3-$ groups in SDAA. This result indicated the adsorption of SDAA onto the fluorite surface. Meanwhile, other new peaks appeared at 1633.7 cm^{-1} and 1543.1 cm^{-1} which were attributed to the $-\text{CON}-$ and $-\text{COO}-$ groups. Compared to the original peaks of $-\text{CON}-$ and $-\text{COO}-$ in SDAA, the peaks of $-\text{CON}-$ and $-\text{COO}-$ on fluorite had an obvious chemical shift after the interaction between fluorite and SDAA, illustrating that SDAA had a strong physical or chemical adsorption on the fluorite surface.

After the treatment of SDAA, there were no characteristic peaks of functional groups of SDAA on the scheelite surface, indicating that SDAA had a weak interaction with the scheelite surface. The above results are in line with the flotation tests (Figures 2–4).

3.5. Calculation Analyses

In order to further explore the interaction mechanism of SDAA and Ca atoms on the surfaces of fluorite and scheelite, the adsorption models of SDAA on the commonly exposed surfaces of fluorite (111) and scheelite (112) were calculated. Adsorption energy is an effective index to characterize the adsorption strength between the collector molecule and the mineral surface. The more negative the adsorption energy is, the easier the reagent adsorbs onto the mineral surface, and the stronger the chemical interaction between the reagent and the mineral surface is. Moreover, the shorter the bond length between the reagent and the active site on the mineral surface is, the more stable the adsorption configuration is. Figure 8 and Table 2 show the optimized adsorption configuration and adsorption energy values of SDAA on the commonly exposed surfaces of fluorite and scheelite, respectively.

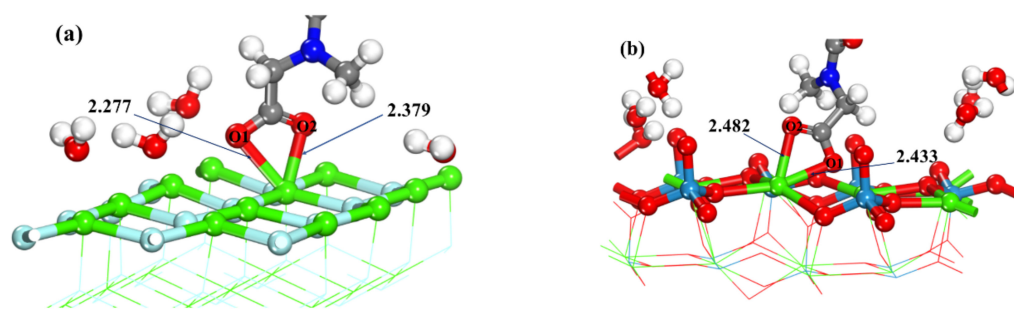


Figure 8. (a) Adsorption configuration of SDAA on fluorite (111) surface and (b) adsorption configuration of SDAA on scheelite (112) surface.

Table 2. Mulliken charge population of active O and Ca atoms before and after SDAA reacting with fluorite and scheelite.

| Fluorite (111) + SDAA | | | | Scheelite (112) + SDAA | | | |
|-----------------------|--------|----------|------------|------------------------|--------|----------|------------|
| Atom | State | Charge/e | Δ/e | Atom | State | Charge/e | Δ/e |
| O1 | Before | −0.57 | −0.15 | O1 | Before | −0.57 | −0.12 |
| | After | −0.72 | | | After | −0.69 | |
| O2 | Before | −0.59 | −0.06 | O2 | Before | −0.59 | −0.03 |
| | After | −0.65 | | | After | −0.62 | |
| Ca | Before | 0.77 | +0.56 | Ca | Before | 1.44 | +0.01 |
| | After | 1.33 | | | After | 1.45 | |

The results of the adsorption energy of SDAA on the fluorite (111) surface was -325.21 kcal/mol, which was far less than that (-87.89 kcal/mol) on the scheelite (112) surface, revealing that SDAA was more easily adsorbed onto the fluorite surface. Moreover, it can be seen from Figure 8 that the carboxyl O of SDAA reacted chemically with the Ca atoms on the surfaces of fluorite and scheelite. The Ca-O bond lengths on fluorite were 2.379 Å and 2.277 Å, respectively, which were shorter than those on scheelite (2.482 Å and 2.433 Å), indicating that SDAA adsorbed more firmly on the fluorite surface.

In addition, the Mulliken charge could further reflect the directions and amounts of electron transfer and the intensity of the chemical reaction between SDAA and the two minerals [45]. Therefore, the Mulliken charge on the fluorite and scheelite surfaces was calculated, as shown in Table 2.

Table 2 further reveals the specific amounts of charge transfer between O atoms and Ca atoms. When SDAA adsorbed onto the fluorite surface, the Mulliken charge of O1 and

O2 (reaction atoms in SDAA) decreased from $-0.57 e$ and $-0.59 e$ to $-0.72 e$ and $-0.65 e$, respectively, with absolute values of $0.15 e$ and $0.06 e$, respectively. The Mulliken charges of Ca on the fluorite surface increased from $0.77 e$ to $1.33 e$, with an absolute value of $0.56 e$. When SDAA was adsorbed on the scheelite surfaces, the Mulliken charges of O1 and O2 in SDAA also decreased, with an absolute value of $0.12 e$ and $0.03 e$, respectively. Moreover, the Mulliken charges of Ca on the scheelite surface increased, with an absolute value of $0.01 e$. Furthermore, the surface activity of fluorite was higher than that of scheelite, since the charge ($0.77 e$) of Ca atoms on the surface of fluorite was smaller than that ($1.44 e$) of Ca atoms on the surface of scheelite. These results indicate that electrons were transferred from Ca on the surfaces of fluorite and scheelite to O1 and O2 in SDAA through surface chemical reactions. However, the amount of electron transfer of Ca on the fluorite surface was much more than that on the scheelite surface, indicating that the chemical reaction between fluorite and SDAA was stronger, which was consistent with the results of the FTIR and zeta potential tests (Figures 6 and 7).

4. Discussion

A new collector SDAA was applied to the selective reverse flotation of fluorite from scheelite. The results of minerals flotation tests showed that under the 1.6×10^{-5} mol/L SDAA at pH 7.0, the selective separation of fluorite against scheelite could be achieved and both high-grade scheelite tailing and fluorite concentrate could be obtained. Additionally, the recovery of fluorite was sensitive to the changes in the pulp pH of more than 9.0. The reason may be that fluorite has a preferable hydrogen bonding ability, making it more sensitive to changes in the solvent environment. The actual flotation tests showed that SDAA can separate fluorite from scheelite without any depressants under the concentration of 100 g/t and pH of 7.0.

When the concentration of SDAA was the same and at pH 7.0, the adsorption density of SDAA on fluorite (0.053 mg/g) was much higher than that on scheelite (0.014 mg/g), indicating the strong adsorption between SDAA and the fluorite surface, which was also consistent with the phenomenon that the recovery of fluorite was much higher than that of scheelite in the single-mineral flotation tests.

The results of the zeta potential tests further showed that NaOL strongly adsorbed onto the surfaces of both fluorite and scheelite, which makes the surface zeta potential values of the two minerals move significantly negatively, while SDAA only made the zeta potential value of fluorite move significantly negatively. There was no obvious change in the zeta potential of scheelite before and after adding SDAA, indicating that NaOL had the strong adsorption interaction on both the fluorite and scheelite surfaces, while SDAA only had the strong adsorption interaction on the fluorite surface.

Furthermore, some typical FTIR bands of SDAA found on the fluorite surface indicated extremely strong adsorption or reaction between SDAA and fluorite. The peaks at 1608.6 and 1394.5 cm^{-1} correspond to the carbonyl stretching vibration of the carboxyl ($-\text{COO}-$) group, which could adsorb onto the fluorite surface and lower the zeta potential of the fluorite surface. Moreover, the peak at 1631.7 cm^{-1} is attributed to an amide group ($-\text{CON}-$), which has a stronger adsorption effect with fluorite compared to scheelite [10]. However, on the surface of the scheelite, the vibrational bands showed no perceptible change, meaning that SDAA had almost no adsorption on the surface of the scheelite. Finally, these results were consistent with the results of zeta potential tests and adsorption capacity tests.

DFT calculations revealed the mechanism of SDAA's selective separation of fluorite and scheelite. According to the literature, the fluorite surface is positively charged at pH 6.0–9.0, while the scheelite surface is always negatively charged [46]. Moreover, the interaction of the amide group which forms a Ca-Amide complex by monodentate coordination is significantly stronger with fluorite than with scheelite [10,25]. At pH 7.0, the chelating sites of SDAA were negatively charged. Therefore, the electrostatic repulsion between SDAA and the surface of the scheelite was not conducive to the adsorption of

SDAA, while the electrostatic repulsion between SDAA and fluorite is beneficial to the adsorption of SDAA. Therefore, the adsorption energy and electron transfer between SDAA and fluorite are greater than those between SDAA and scheelite.

Additionally, the Ca density was determined to be $12.87 \mu\text{mol}/\text{m}^2$ on the fluorite (111) surface and $6.58 \mu\text{mol}/\text{m}^2$ on the scheelite (112) surface, respectively, according to the previous literature [37,42]. A higher Ca density on the fluorite surface can accommodate more SDAA species for adsorption, while the lower density on the surface of scheelite cannot accommodate enough SDAA species for adsorption.

5. Conclusions

For the first time, fluorite could be selectively and effectively separated from scheelite by using SDAA as a collector without any depressants through the flotation tests of the single mineral, binary mixed minerals, and actual ore. Surface adsorption and zeta potential tests indicate that SDAA strongly adsorbs onto the surface of fluorite but hardly adsorbs on the scheelite surface. The results of the FTIR tests further prove that the carboxyl group of SDAA has a stronger chemical interaction with the fluorite surface than the scheelite surface, leading to a decrease in the zeta potential value on the fluorite surface after SDAA adsorption. DFT and crystal chemistry calculations further indicate that the Ca atoms on the fluorite surface have a higher density and activity, which makes SDAA interact more strongly with fluorite. Therefore, the significant difference in the adsorption behavior of the amino acid surfactant SDAA on the surfaces of fluorite and scheelite provides the possibility for the efficient separation of fluorite from scheelite in industry.

Author Contributions: Conceptualization, Z.M. and L.T.; methodology, Z.M. and Z.J.; software, Z.M. and L.T.; validation, Z.M. and T.P.; formal analysis, Z.M. and J.W.; investigation, Z.M. and L.T.; resources, W.S. and Z.G.; data curation, Z.M. and L.T.; writing—original draft preparation, Z.M.; writing—review and editing, Z.M. and Z.G.; visualization, Z.M., L.T. and Z.G.; supervision, Z.G.; project administration, Z.G.; funding acquisition, Z.G. All authors have read and agreed to the published version of the manuscript.

Funding: The authors acknowledge financial support from the Key Research and Development Program of Hunan Province, China (2021SK2043), the Leading Talents of S&T Innovation of Hunan Province, China (2021RC4002), the Science Fund for Distinguished Young Scholars of Hunan Province, China (2020JJ2044), the National 111 Project, China (B14034), and the Fundamental Research Funds for the Central Universities of Central South University (2021zzts0908).

Data Availability Statement: Not applicable.

Acknowledgments: This work was carried out in part using hardware and software provided by the High-Performance Computing Centers of Central South University.

Conflicts of Interest: The authors declare no conflict of interest.

References

1. Wang, J.; Gao, Z.; Han, H.; Sun, W.; Gao, Y.; Ren, S. Impact of NaOL as an accelerator on the selective separation of scheelite from fluorite using a novel self-assembled Pb-BHA-NaOL collector system. *Appl. Surf. Sci.* **2020**, *537*, 147778. [[CrossRef](#)]
2. Gao, Z.; Deng, J.; Sun, W.; Wang, J.; Liu, Y.; Xu, F.; Wang, Q. Selective Flotation of Scheelite from Calcite Using a Novel Reagent Scheme. *Miner. Process. Extr. Metall. Rev.* **2020**, *43*, 1–13. [[CrossRef](#)]
3. Wang, J.; Li, W.; Zhou, Z.; Gao, Z.; Hu, Y.; Sun, W. 1-Hydroxyethylidene-1,1-diphosphonic acid used as pH-dependent switch to depress and activate fluorite flotation I: Depressing behavior and mechanism. *Chem. Eng. Sci.* **2020**, *214*, 115369. [[CrossRef](#)]
4. Gao, Y.; Fu, X.; Yue, T.; Sun, W. A novel GCMS method for the quantitative analysis of sodium oleate in froth flotation. *Miner. Eng.* **2021**, *176*, 107317. [[CrossRef](#)]
5. Kupka, N.; Rudolph, M. Froth flotation of scheelite—A review. *Int. J. Min. Sci. Technol.* **2018**, *28*, 373–384. [[CrossRef](#)]
6. Gao, Z.; Bai, D.; Sun, W.; Cao, X.; Hu, Y. Selective flotation of scheelite from calcite and fluorite using a collector mixture. *Miner. Eng.* **2015**, *72*, 23–26. [[CrossRef](#)]
7. Wang, R.; Wei, Z.; Han, H.; Sun, W.; Hu, Y.; Wang, J.; Wang, L.; Liu, H.; Yang, Y.; Zhang, C.; et al. Fluorite particles as a novel calcite recovery depressant in scheelite flotation using Pb-BHA complexes as collectors. *Miner. Eng.* **2018**, *132*, 84–91. [[CrossRef](#)]
8. Chen, W.; Feng, Q.; Zhang, G.; Yang, Q.; Zhang, C.; Xu, F. The flotation separation of scheelite from calcite and fluorite using dextran sulfate sodium as depressant. *Int. J. Miner. Process.* **2017**, *169*, 53–59. [[CrossRef](#)]

9. Zhang, Z.; Cao, Y.; Ma, Z.; Liao, Y. Impact of calcium and gypsum on separation of scheelite from fluorite using sodium silicate as depressant. *Sep. Purif. Technol.* **2019**, *215*, 249–258. [[CrossRef](#)]
10. Gao, Z.; Jiang, Z.; Sun, W.; Pooley, S.G.; Wang, J.; Liu, Y.; Xu, F.; Wang, Q.; Zeng, L.; Wu, Y. New role of the conventional foamer sodium *N*-lauroylsarcosinate as a selective collector for the separation of calcium minerals. *J. Mol. Liq.* **2020**, *318*, 114031. [[CrossRef](#)]
11. Zhang, Y.; Li, Y.; Chen, R.; Wang, Y.; Deng, J.; Luo, X. Flotation Separation of Scheelite from Fluorite Using Sodium Polyacrylate as Inhibitor. *Minerals* **2017**, *7*, 102. [[CrossRef](#)]
12. Chen, W.; Feng, Q.; Zhang, G.; Yang, Q.; Zhang, C. The effect of sodium alginate on the flotation separation of scheelite from calcite and fluorite. *Miner. Eng.* **2017**, *113*, 1–7. [[CrossRef](#)]
13. Liu, J.; Wang, X.; Zhu, Y.; Han, Y. Flotation separation of scheelite from fluorite by using DTPA as a depressant. *Miner. Eng.* **2021**, *175*, 107311. [[CrossRef](#)]
14. Alzobaidi, S.; Wu, P.; Da, C.; Zhang, X.; Hackbarth, J.; Angeles, T.; Rabat-Torki, N.J.; MacAuliffe, S.; Panja, S.; Johnston, K.P. Effect of surface chemistry of silica nanoparticles on contact angle of oil on calcite surfaces in concentrated brine with divalent ions. *J. Colloid Interface Sci.* **2020**, *581*, 656–668. [[CrossRef](#)]
15. Bikina, P.K. Contact angle measurements of CO₂-water-quartz/calcite systems in the perspective of carbon sequestration. *Int. J. Greenh. Gas Control* **2011**, *5*, 1259–1271. [[CrossRef](#)]
16. Zhao, J.; Yao, G.; Wen, D. Salinity-dependent alterations of static and dynamic contact angles in oil/brine/calcite systems: A molecular dynamics simulation study. *Fuel* **2020**, *272*, 117615. [[CrossRef](#)]
17. Zawala, J.; Drzymala, J.; Malysa, K. An investigation into the mechanism of the three-phase contact formation at fluorite surface by colliding bubble. *Int. J. Miner. Process.* **2008**, *88*, 72–79. [[CrossRef](#)]
18. Gao, Y.; Gao, Z.; Sun, W.; Hu, Y. Selective flotation of scheelite from calcite: A novel reagent scheme. *Int. J. Miner. Process.* **2016**, *154*, 10–15. [[CrossRef](#)]
19. Zhang, W.; Feng, Z.; Yang, Y.; Sun, W.; Pooley, S.; Cao, J.; Gao, Z. Bi-functional hydrogen and coordination bonding surfactant: A novel and promising collector for improving the separation of calcium minerals. *J. Colloid Interface Sci.* **2020**, *585*, 787–799. [[CrossRef](#)]
20. Waller, E.H.; Dix, S.; Gutsche, J.; Widera, A.; von Freymann, G. Functional Metallic Microcomponents via Liquid-Phase Multiphoton Direct Laser Writing: A Review. *Micromachines* **2019**, *10*, 827. [[CrossRef](#)]
21. Qi, C.; Liu, L.; He, J.; Chen, Q.; Yu, L.-J.; Liu, P. Understanding Cement Hydration of Cemented Paste Backfill: DFT Study of Water Adsorption on Tricalcium Silicate (111) Surface. *Minerals* **2019**, *9*, 202. [[CrossRef](#)]
22. Lay, C.L.; Koh, C.S.L.; Lee, Y.H.; Phan-Quang, G.C.; Sim, H.Y.F.; Leong, S.X.; Han, X.; Phang, I.Y.; Ling, X.Y. Two-Photon-Assisted Polymerization and Reduction: Emerging Formulations and Applications. *ACS Appl. Mater. Interfaces* **2020**, *12*, 10061–10079. [[CrossRef](#)]
23. Wei, Z.; Sun, W.; Hu, Y.; Han, H.; Sun, W.; Wang, R.; Zhu, Y.; Li, B.; Song, Z. Structures of Pb-BHA Complexes Adsorbed on Scheelite Surface. *Front. Chem.* **2019**, *7*, 645. [[CrossRef](#)]
24. Yang, B.; Yin, W.; Zhu, Z.; Sun, H.; Sheng, Q.; Fu, Y.; Yao, J.; Zhao, K. Differential adsorption of hydrolytic polymaleic anhydride as an eco-friendly depressant for the selective flotation of apatite from dolomite. *Sep. Purif. Technol.* **2020**, *256*, 117803. [[CrossRef](#)]
25. Zhang, W.; Feng, Z.; Mulenga, H.; Sun, W.; Cao, J.; Gao, Z. Synthesis of a novel collector based on selective nitrogen coordination for improved separation of galena and sphalerite against pyrite. *Chem. Eng. Sci.* **2020**, *226*, 115860. [[CrossRef](#)]
26. Wu, J.; Ma, W.; Wang, X.; Jiao, F.; Qin, W. The effect of galvanic interaction between chalcopyrite and pyrite on the surface chemistry and collector adsorption: Flotation and DFT study. *Colloids Surf. A Physicochem. Eng. Asp.* **2020**, *607*, 125377. [[CrossRef](#)]
27. Clark, S.J.; Segall, M.D.; Pickard, C.J.; Hasnip, P.J.; Probert, M.I.; Refson, K.; Payne, M.C. Payne, first principles methods using CASTEP. *Z. Kristallogr. Cryst. Mater.* **2005**, *220*, 567–570. [[CrossRef](#)]
28. Gao, Z.-Y.; Sun, W.; Hu, Y.-H.; Liu, X. Surface energies and appearances of commonly exposed surfaces of scheelite crystal. *Trans. Nonferrous Met. Soc. China* **2013**, *23*, 2147–2152. [[CrossRef](#)]
29. Yu, S.; Zhang, C.; Ma, L.; Fang, Q.; Chen, G. Insight into As₂O₃ adsorption characteristics by mineral oxide sorbents: Experimental and DFT study. *Chem. Eng. J.* **2020**, *420*, 127593. [[CrossRef](#)]
30. He, J.; Zhang, H.; Yue, T.; Sun, W.; Hu, Y.; Zhang, C. Effects of Hydration on the Adsorption of Benzohydroxamic Acid on the Lead-Ion-Activated Cassiterite Surface: A DFT Study. *Langmuir* **2021**, *37*, 2205–2212. [[CrossRef](#)]
31. Foroutan, A.; Abadi, M.A.Z.H.; Kianinia, Y.; Ghadiri, M. Critical importance of pH and collector type on the flotation of sphalerite and galena from a low-grade lead–zinc ore. *Sci. Rep.* **2021**, *11*, 1–11.
32. Vieira, A.M.; Peres, A.E. The effect of amine type, pH, and size range in the flotation of quartz. *Miner. Eng.* **2007**, *20*, 1008–1013. [[CrossRef](#)]
33. Hoseinian, F.S.; Rezai, B.; Kowsari, E.; Safari, M. Kinetic study of Ni(II) removal using ion flotation: Effect of chemical interactions. *Miner. Eng.* **2018**, *119*, 212–221. [[CrossRef](#)]
34. Abaka-Wood, G.B.; Zanin, M.; Addai-Mensah, J.; Skinner, W. The upgrading of rare earth oxides from iron-oxide silicate rich tailings: Flotation performance using sodium oleate and hydroxamic acid as collectors. *Adv. Powder Technol.* **2018**, *29*, 3163–3172. [[CrossRef](#)]
35. Abaka-Wood, G.B.; Addai-Mensah, J.; Skinner, W. A study of flotation characteristics of monazite, hematite, and quartz using anionic collectors. *Int. J. Miner. Process.* **2017**, *158*, 55–62. [[CrossRef](#)]

36. Zhu, H.; Qin, W.; Chen, C.; Chai, L.; Jiao, F.; Jia, W. Flotation separation of fluorite from calcite using polyaspartate as depressant. *Miner. Eng.* **2018**, *120*, 80–86. [[CrossRef](#)]
37. Gao, Y.; Gao, Z.; Sun, W.; Yin, Z.; Wang, J.; Hu, Y. Adsorption of a novel reagent scheme on scheelite and calcite causing an effective flotation separation. *J. Colloid Interface Sci.* **2017**, *512*, 39–46. [[CrossRef](#)]
38. Jong, K.; Paek, I.; Kim, Y.; Li, I.; Jang, D. Flotation mechanism of a novel synthesized collector from *Evodiaefructus* onto fluorite surfaces. *Miner. Eng.* **2019**, *146*, 106017. [[CrossRef](#)]
39. Cao, Z.; Cao, Y.; Qu, Q.; Zhang, J.; Mu, Y. Separation of bastnäsite from fluorite using ethylenediamine tetraacetic acid as depressant. *Miner. Eng.* **2019**, *134*, 134–141. [[CrossRef](#)]
40. Rubio, L.; Alonso, C.; Rodríguez, G.; Cócera, M.; López-Iglesias, C.; Coderch, L.; De la Maza, A.; Parra, J.; López, O. Bicellar systems as new delivery strategy for topical application of flufenamic acid. *Int. J. Pharm.* **2013**, *444*, 60–69. [[CrossRef](#)]
41. Pujari, S.P.; van Andel, E.; Yaffe, O.; Cahen, D.; Weidner, T.; van Rijn, C.; Zuilhof, H. Mono-Fluorinated Alkyne-Derived SAMs on Oxide-Free Si(111) Surfaces: Preparation, Characterization and Tuning of the Si Workfunction. *Langmuir* **2013**, *29*, 570–580. [[CrossRef](#)]
42. Jiang, W.; Gao, Z.; Khoso, S.A.; Gao, J.; Sun, W.; Pu, W.; Hu, Y. Selective adsorption of benzhydroxamic acid on fluorite rendering selective separation of fluorite/calcite. *Appl. Surf. Sci.* **2017**, *435*, 752–758. [[CrossRef](#)]
43. Müller, M.; Wirth, L.; Urban, B. Determination of the Carboxyl Dissociation Degree and pK a Value of Mono and Polyacid Solutions by FTIR Titration. *Macromol. Chem. Phys.* **2021**, *222*, 2000334. [[CrossRef](#)]
44. Tran, T.L.N.; Miranda, A.F.; Mouradov, A.; Adhikari, B. Physicochemical Characteristics of Protein Isolated from Thraustochytrid Oilcake. *Foods* **2020**, *9*, 779. [[CrossRef](#)]
45. Zhang, W.; Cao, J.; Wu, S.; Sun, W.; Feng, Z.; Gao, Z. Synthesis of selective heteroatomic collectors for the improved separation of sulfide minerals. *Sep. Purif. Technol.* **2022**, *287*, 120563. [[CrossRef](#)]
46. Miller, J.; Fa, K.; Calara, J.; Paruchuri, V. The surface charge of fluorite in the absence of surface carbonation. *Colloids Surf. A Physicochem. Eng. Asp.* **2004**, *238*, 91–97. [[CrossRef](#)]